Cell and Tissue Research (2019) 375:345–357
https://doi.org/10.1007/s00441-018-2925-8

REGULAR ARTICLE

Development of nNOS-positive preganglionic sympathetic neurons in the rat thoracic spinal cord

Konstantin Y. Moiseev[1] · Irina V. Romanova[2] · Andrey P. Masliukov[3] · Petr M. Masliukov[1]

Received: 11 January 2018 / Accepted: 10 September 2018 / Published online: 28 September 2018

Abstract

To gain a better understanding of the neuroplasticity of sympathetic neurons during postnatal ontogenesis, the distribution of neuronal nitric oxide synthase (nNOS) immunoreactivity was studied in sympathetic preganglionic neurons (SPN) in the spinal cord (Th2 segment) of female Wistar rats at different ages (newborn, 10-, 20-, 30-day-old; 2-, 6-month-old; 3-year-old). In all age groups, the majority of nNOS-immunoreactive (IR) neurons was observed in the nucleus intermediolateralis thoracolumbalis pars principalis. In the first month, the proportion of nNOS-IR neurons decreased significantly from 92 ± 3.4% in newborn to 55 ± 4.6% in 1-month-old, while the number of choline acetyltransferase (ChAT)-IR neurons increased from 74 ± 4.2% to 99 ± 0.3% respectively. Decreasing nNOS expression in the first 10 days of life was also confirmed by western blot analysis. Some nNOS-IR SPN also colocalized calbindin (CB) and cocaine and amphetamine-regulated transcript (CART). The percentage of NOS(+)/CB(−) SPN increased from 23 ± 3.6% in 10-day-old to 36 ± 4.2% in 2-month-old rats. Meanwhile, the proportion of NOS(+)/CART(−) neurons decreased from 82 ± 4.7% in newborn to 53 ± 6.1% in 1-month-old rats. The information provided here will also serve as a basis for future studies investigating the mechanisms of autonomic neuron development.

Keywords Spinal cord · Sympathetic preganglionic neurons · Nitric oxide synthase · Development · Immunohistochemistry

Introduction

In the spinal cord (SC), the sympathetic preganglionic neurons (SPN) mostly use acetylcholine as their main neurotransmitter. Cholinergic neurons are identified reliably by immunohistochemical detection of the acetylcholine-synthesizing enzyme, choline acetyltransferase (ChAT) (Barber et al. 1984; Wetts and Vaughn 1994). Many cholinergic SPN also express neuronal nitric oxide synthase (nNOS) (Anderson 1992; Grkovic and Anderson 1997).

nNOS is expressed in the central and peripheral nervous system and predominantly produces nitric oxide (NO) in neuronal tissues. NO is a diffusible molecule that acts in various physiologic and pathophysiologic processes (Snyder 1992; Meller and Gebhart 1993; Prast and Philippu 2001; Petho and Reeh 2012). Neurons that generate NO can also be identified by NADPH diaphorase (NADPH-d) histochemistry (Dawson et al. 1991; Schmidt et al. 1992; Wetts and Vaughn 1994).

In addition to nNOS, many preganglionic neurons are also immunoreactive (IR) to the neuropeptide cocaine and amphetamine-regulated transcript (CART) and calcium-binding proteins calbindin (CB) and calretinin (Grkovic and Anderson 1997; Dun et al. 2000; Fenwick et al. 2006). CART immunoreactivity selectively identifies cardiovascular SPN. The numbers of CB-IR and CART-IR SPN peaked in the thoracic region (Gonsalvez et al. 2010). The majority of CB-IR SPN also had colocalized nNOS, although a population of preganglionic neurons expressed only CB immunoreactivity. CB-IR SPN send their axons to the superior cervical and stellate ganglia (Grkovic and Anderson 1997).

The expression of the spectrum of neurotransmitters in sympathetic ganglionic neurons is subject to changes during pre- and postnatal development (Young et al. 2011; Masliukov et al. 2015, 2016). NO also plays a developmental role in regulating synapse formation and patterning (Gibbs 2003).

✉ Petr M. Masliukov
mpm@yma.ac.ru

[1] Department of Normal Physiology and Biophysics, Yaroslavl State Medical University, Revoliucionnaya 5, Yaroslavl, Russia 150000

[2] Sechenov Institute of Evolutionary Physiology and Biochemistry of the Russian Academy of Sciences, St. Petersburg, Russia

[3] I.M. Sechenov First Moscow State Medical University, Moscow, Russia

Recent studies suggest that NO may also mediate the switch from proliferation to differentiation during neurogenesis (Cossenza et al. 2014; Dawson and Dawson 2018). However, there are only limited data about NO synthesis or nNOS expression in the development of autonomic neurons. In the spinal cord of zebrafish embryos, NADPH-d staining decreases after secondary patterning of ventral motor neurons is complete (Gibbs 2003). on the other hand, preganglionic NADPH-d-positive fibers were absent in sympathetic ganglia in newborns and their density increased in the early development in rodents (Emanuilov et al. 2008).

Thus, in order to better understand the development of NO-ergic system in the autonomic nervous system at different levels, the purpose of this study is to investigate the development of nNOS-IR SPN in rats of different ages from newborn through senescence using immunohistochemistry, colocalization study with other neurochemicals and western blot analysis. Since the Th2 segment is the major source of preganglionic fibers to cranial sympathetic ganglia (superior cervical and stellate) and CB-IR, CR-IR neurons, we studied the SC at this level.

Experimental procedures

Animals

All animal procedures were approved by the Institutional Animal Care and Use Committee of the Yaroslavl State Medical University and were conducted in accordance with the "Guide for the Care and Use of Laboratory Animals" (NIH Publication No. 85–23, revised 1996) as well as the relevant Guidelines of the Russian Ministry of Health for scientific experimentation on animals. All efforts were made to minimize the number of animals and their suffering throughout the experiment.

Newborn (body weight 5–7 g), 10-day-old (body weight 15–25 g), 20-day-old (body weight 35–55 g) 30-day-old (body weight 70–90 g), 2-month-old (body weight 160–190 g), 6-month-old (body weight 260–280 g), and 3-year-old (body weight 310–330 g) female Wistar rats (seven groups each containing ten animals (five for immunohistochemistry and five for Western blotting)) were used in this work to study. All animals were kept in acrylic cages with wood shavings in an acclimatized room (12/12-h light/dark cycle; 22 ± 3 °C) with free access to food and water.

Immunohistochemistry

All animals were sacrificed with a lethal dose of sodium pentobarbital (Nembutal®, 300 mg/kg, i.p.), after which they were perfused transcardially with 20 ml (newborn and 10-day-old), 100 ml (20- and 30-day-old), or 500 ml (2-month-old and older) of physiological saline and 1 ml heparin followed by a similar volume of fixative composed of 4% paraformaldehyde (PF) in 0.1 M phosphate buffer.

After perfusion, the cervical and thoracic region of the SC was removed by laminectomy. In animals of all age groups, the Th2 segment of the SC was defined by counting the appropriate number of nerve roots. Then, the Th2 segment was dissected, rinsed in physiological solution and immersed in 4% PF for 1–2 h at room temperature. No other segments were studied.

Following fixation, Th2 segments of the SC were washed in three 30-min changes of phosphate-buffered saline (PBS; 0.01 M; pH 7.4), cryoprotected by overnight immersion in 20% buffered (pH 7.4) sucrose solution at 4 °C, mounted in TissueTek (Sakura Finetek Europe, Zoeterwoude, the Netherlands) on a cryostat chuck and frozen. Twelve-micrometer-thick cross-sections were cut with a cryostat, mounted on poly-L-lysine-coated slides and air-dried for 1 h.

Transverse serial sections of the SC were processed for immunohistochemistry. The sections were preincubated for 30 min at room temperature with blocking buffer containing 5% normal donkey serum (Jackson ImmunoResearch Laboratories, USA) and 0.3% Triton X-100 (Sigma, USA) in PBS to prevent the non-specific binding of secondary antibodies. To visualize NOS(+), ChAT(+), CB(+) and CART(+) neurons, single or double immunostaining with antibodies (raised in different host species; see Table 1) was performed. nNOS+ChAT, nNOS+CB and nNOS+CART combination of antibodies was used.

Next, the sections were incubated in the primary antisera for 24 h at room temperature, rinsed in PBS and further incubated in the corresponding secondary antisera (see Table 2) for 2 h at room temperature. The sections were then rinsed three final times in PBS, mounted on glass slides, allowed to dry overnight and coverslipped using VectaShield (Vector Bioproducts, USA). For the antibody specificity, the controls were preabsorbed with the primary antibody to the nNOS-immunogenic peptide (Abcam, ab22863) or the omission of the primary antibody.

Western blot analysis

All experimental rats were anesthetized with a lethal dose of sodium pentobarbital (Nembutal®, 300 mg/kg, i.p.). The SC was rapidly removed by laminectomy in animals of all age groups and placed on ice. the Th2 segment of the SC was studied. It was identified with the same procedure as for fixed SC—by counting the number of dorsal roots.

Since the main number of SPN was found in the intermediate zone, the middle third of SPN between the dorsal and ventral horn was taken for the study. Under a dissection microscope, we separated the intermediate zone with the lateral horn and central channel area with two parallel longitudinal

Table 1 Primary antisera used for immunohistochemistry

Primary antisera	Host species	Dilution	Source
nNOS	Goat	1:300	Abcam, ab1376
nNOS	Rabbit	1:50	LifeSpan BioSciences, LS-B8696
ChAT	Goat	1:50	Millipore, AB144P
CB	Rabbit	1:500	Abcam, ab11426
CART	Rabbit	1:500	Phoenix PhaIncorp, H-003-62

incisions by a microtome blade in order to keep all autonomic nuclei (ILP, ILf, IC, and ICPe) and not to take non-autonomic nNOS-IR neurons from dorsal and ventral horns.

Samples from spinal cord were homogenized with a lysis buffer (20 mM Tris HCl, 150 mM NaCl, 1 mM EDTA, 1 mM EGTA, 1% Triton X-100, protease inhibitor cocktail (Sigma)). The concentration of the total proteins was determined in all lysed tissues using the Bradford reagent (Fermentas, USA). Forty micrograms of protein was loaded per well. Each tissue lysate was diluted in sample buffer (Bio-Rad Laboratories Inc., USA) and denatured at 95 °C for 5 min. Seven samples (one from each time point) were processed together. Equivalent amounts of samples were loaded and separated by 10% polyacrylamide gel electrophoresis and transferred to PVDF transfer membranes (AppliChem, Germany). Membranes were blocked with a blocking solution containing 3% non-fat dry milk (AppliChem, Germany) in TBS-T (0.1% Tween 20, 0.2 mM Tris, 137 mM NaCl) for 30 min at room temperature. After washing with TBS-T, membranes were incubated with primary antibodies (rabbit anti-nNOS, 1:1000, LS-B8696, LifeSpan BioSciences; rabbit anti-GAPDH (Glyceraldehyde 3-phosphate dehydrogenase), 1:2500, ab9485, Abcam) diluted in the same blocking solution at 4 °C overnight. Following washing with TBS-T, membranes were incubated with secondary antibodies (goat HRP-conjugated anti-rabbit IgG, Abcam, ab6721) at 1:3000. The immunoblots were detected by chemiluminescence (ECL Prime Western blotting detection reagent, BioRad) with a Syngene G:BOX Chemi XR5E imaging system (Syngene, UK). Chemiluminescent signals were quantified with Gene Tools Gel Analysis software (Syngene, UK), and expressed relative to GAPDH. Protein molecular weight markers were included in each Western blot analysis.

Image processing and statistics

The specimens were examined using an Olympus BX43 fluorescence microscope (Tokyo, Japan) fitted with filter sets that allowed separate visualization of FITC and CY3. Images from the fluorescence microscope were recorded using a TCH 5.0 cooled CCD digital camera and ISCapture version 3.6 for Windows imaging software (Tucsen, China). Each image was processed using a sharpen filter and contrast and brightness adjustment only. All photomicrographic plates were created using Adobe Photoshop 6.0 software (Adobe Systems, USA).

To calculate the percentage of IR neurons, transverse sections were taken from the SC at a distance of approximately 0.05 mm. In our earlier works, we did not find differences in the percentage and soma size between nNOS-IR neurons located in the left and right dorsal root ganglia (Masliukov et al. 2014). Thus, data from the right and left spinal halves were averaged. We did not study rostro-caudal representation and cells were counted on randomly chosen SC sections.

To avoid duplicate counts of neurons in the serial sections, only those nerve cell bodies containing a clearly identified nucleus were counted in any given section. To determine the percentage of IR profiles, we counted the total number of IR neurons in the section and considered them as 100%. The data from ten sections in each animal from each age group were included in this study. The data from each age group were averaged, yielding group sizes of $n = 5$. The cross-sectional areas of 100 nNOS-IR profiles were measured in random order in each nuclei in each age group using ImageJ software (http://imagej.nih.gov/ij/index.html). All analyses were carried out with the observer blind to the groupings.

The statistical methods include the calculation of the mean and standard error of the mean (SEM). The differences in the

Table 2 Secondary antisera used for immunohistochemistry

Secondary antisera	Dilution	Source
Donkey anti-goat IgG FITC	1:200	Jackson Immunoresearch, 705-095-147
Donkey anti-goat IgG CY3	1:200	Jackson Immunoresearch, 705-165-147
Donkey anti-rabbit IgG FITC	1:200	Jackson Immunoresearch, 711-095-152
Donkey anti-rabbit IgG CY3	1:200	Jackson Immunoresearch, 711-165-152

CY3 cyanine 3, *FITC* fluorescein isothiocyanate

means were subjected to one-way ANOVA, followed by Tukey's post-test of multiple comparisons. Differences were considered statistically significant if $p < 0.05$.

In the text, the binding or immunoreactivity of a marker molecule in a profile has been designated with a plus sign (e.g., nNOS(+)); conversely, the absence of binding or immunoreactivity has been indicated with a minus sign (e.g., nNOS(−)).

Results

Immunohistochemistry and western blot analysis were used to label nNOS-IR SPN in the Th2 segment of the SC from rats of different ages. Immunoreactivity to nNOS was mainly detected in the cell bodies of neurons bilaterally located in the lateral horns of the spinal cord.

Immunohistochemical studies of nNOS-IR SPN

In the spinal cord, nNOS was detected in the lateral horns in the following: (1) nucleus intermediolateralis thoracolumbalis pars principalis (nucl.ILp), (2) nucleus intermediolateralis thoracolumbalis pars funicularis (nucl.ILf), (3) nucleus intercalatus spinalis (nucl.IC) and (4) nucleus intercalatus spinalis pars paraependymalis (nucl.ICpe) from the moment of birth in all animals (Fig. 1a).

In addition to preganglionic neurons, three sparse groups of nNOS-IR neurons were found. These neurons were as follows: (1) partition cells located in the intermediate gray matter, (2) small cells surrounding the ventral part of the central canal, and (3) small neurons located within lamina III–VI of the dorsal horn. Since these three groups are nonautonomic (Wetts et al. 1995), they were excluded from further analysis.

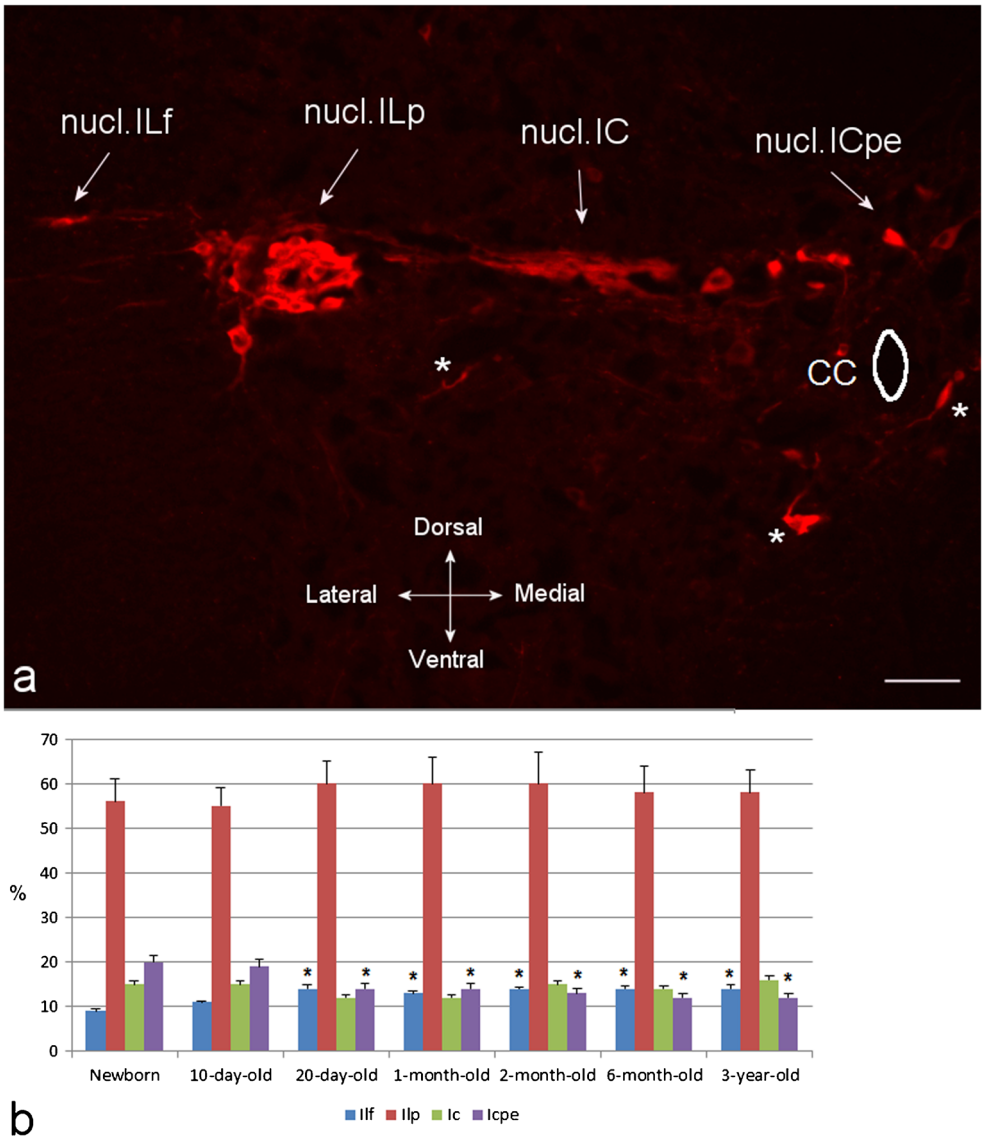

Fig. 1 nNOS-IR SPN in the spinal cord of 20-day-old rat. ILf, the lateral funiculus; ILp, the principal intermediolateral nucleus; IC, the nucleus intercalatus spinalis; ICpe, the nucleus intercalatus pars paraependymalis; CC, the central canal. Non-autonomic neurons are indicated by stars. Bar, 100 μm (**a**). Percentage of nNOS-IR SPN neurons in the ILp, ILf, IC, and ICPe of rats of different ages. The error bars represent SEM (*$p < 0.05$, when comparing to newborn) (**b**)

In all rats, the largest percentage of nNOS-IR neurons was located in nucl.ILp. In the first 30 days, the percentage of NOS-IR neurons in nucl.ILf significantly increased from 9 ± 0.8% in newborns to 14 ± 1.2% ($p < 0.05$) and the proportion of positive cells in the nucl.ICpe significantly decreased from 20 ± 1.8% to 14 ± 0.5% ($p < 0.05$) (Fig. 1b).

In all animals, cells immunoreactive for nNOS showed strong cytoplasmic staining that extended into the proximal dendrites. Most SPN were tightly clustered in the nucl.ILp. Many processes were oriented medially, some extending as far as the ventricle, while other processes extended into the adjacent lateral funiculus. Most of the nNOS-IR neurons had a round or fusiform shape on sections. Also, a triangle shape was observed.

In all four nuclei, the mean of the cross-sectional area of the nNOS-IR SPN profiles significantly increased in the first 10 days of development ($p < 0.05$, Table 3). In the ILp, ILf, IC, and ICpe, the mean of the cross-sectional area of the nNOS-IR SPN profiles were not significantly different between 10-day-old and older rats ($p > 0.05$). We did not observe differences between cross-sectional areas of nNOS-IR neuron profiles in different nuclei ($p > 0.05$).

Colocalization with ChAT

nNOS/ChAT colocalization in the ILp In newborns and 10-day-old rats, the largest percentage of neurons in nucl.ILp was nNOS-IR and also had immunoreactivity to ChAT (Figs. 2 and 3). However, some nNOS-IR neurons in these age groups did not contain ChAT. nNOS(+)/ChAT(−) neurons in newborns and 10-day-old rats were located in the ventral part of the nucl.ILp. In the ILp, the percentage of nNOS-IR neurons decreased and the proportion of ChAT-IR cells increased during the development. In the first month, the proportion of nNOS-IR neurons decreased significantly from 92 ± 3.4% in newborn to 55 ± 4.6% in 1-month-old ($p < 0{,}001$), while the number of ChAT-IR neurons increased from 74 ± 4.2% to 99 ± 0.3% respectively ($p < 0.01$). There were no significant differences in the percentage of nNOS(−)/ChAT(+) neurons between 30-day-old and older rats ($p > 0.05$).

Table 3 Cross-sectional areas of nNOS-IR-neurons (μm²) in the SC ($n = 100$ in every nucleus, every age group)

Age	nucl.ILp	nucl.ILf	nucl.IC	nucl.ICpe
Newborn	176 ± 8	163 ± 11	182 ± 19	166 ± 12
10-day-old	208 ± 14*	215 ± 15*	222 ± 20*	189 ± 17
20-day-old	213 ± 14*	205 ± 9*	218 ± 14*	200 ± 16*
1-month-old	220 ± 13*	214 ± 16*	230 ± 12*	226 ± 18*
2-month-old	225 ± 12*	225 ± 23*	225 ± 19*	225 ± 17*
6-month-old	216 ± 15*	221 ± 18*	218 ± 14*	232 ± 18*
3-year-old	230 ± 28*	212 ± 15*	214 ± 19*	206 ± 32*

* statistically significant differences compared with newborns (*$p < 0.05$)

nNOS/ChAT colocalization in the nucl.ILf In all age groups from newborns to aged rats, 100% of nNOS-IR neurons colocalized ChAT.

nNOS/ChAT colocalization in the nucl.IC and nucl.ICpe In nucl.IC and nucl.ICpe of newborns, the proportion of nNOS(+)/ChAT(−), nNOS(+)/ChAT(+), and nNOS(−)/ChAT(+) neurons was 35 ± 1.7%, 31 ± 1.5%, and 34 ± 1.1% (nucl.IC), 36 ± 2.5%, 31 ± 1.2%, and 33 ± 2.6% (nucl.ICpe) and did not change significantly in the postnatal development ($p > 0.05$) (Table 4).

Colocalization with CB and CART

Many nNOS-IR SPN colocalized CB and CART from the moment of birth. CB-IR cell bodies and their proximal dendrites showed immunoreactivity, which varied in intensity from weak to very strong (Fig. 4). The fluorescent intensity of CART-IR neurons also varied, some CART neurons being faintly and others intensely stained (Fig. 5). The largest percentage of CB-IR and CART-IR neurons colocalizing nNOS was found in the nucl.ILp with a smaller one in the nucl.IC. No colocalization was observed in the nucl.ILf and nucl.ICpe.

nNOS/CB and nNOS/CART colocalization in the nucl.ILp The percentage of nNOS(+)/CB(−) increased from 22 ± 3.3% in newborn and 23 ± 3.6% in 10-day-old rats to 36 ± 4.2% in 2-month-old (statistically significant differences between 10-day-old and 2-month-old rats, $p < 0.05$) (Fig. 2). However, the proportion of nNOS(−)/CB(+) SPN did not change in the first month of life and significantly increased from 8 ± 2.5% in 1-month-old to 17 ± 3.4% in 6-month-old ($p < 0.05$).

Meanwhile, the proportion of nNOS(+)/CART(−) neurons decreased from 82 ± 4.7% in 10-day-old to 53 ± 6.1% in 1-month-old rats ($p < 0.001$) (Fig. 2). Opposite dynamics was shown for nNOS(−)/CART(+) neurons, where the percentage significantly increased from 4 ± 0.9% in 10-day-old to 27 ± 3.7% in 1-month-old animals ($p < 0.001$).

NOS/CB and NOS/CART colocalization in the nucl.IC In the nucl.IC, the percentage of nNOS(+)/CB(+) SPN was high and increased from 40 ± 4.8% in newborn and 43 ± 5.1% in 10-day-old rats until 61 ± 5.5% in 20-day-old rats (statistically significant differences, $p < 0.05$) (Fig. 6a). The proportion of nNOS(+)/CB(−) SPN also increased from 18 ± 2.4% in newborns and 20 ± 2.1% in 10-day-old to 30 ± 3.5% in 20-day-old rats (statistically significant differences, $p < 0.05$). We did not observe statistically significant differences between different 20-day-old and older rats ($p > 0.05$).

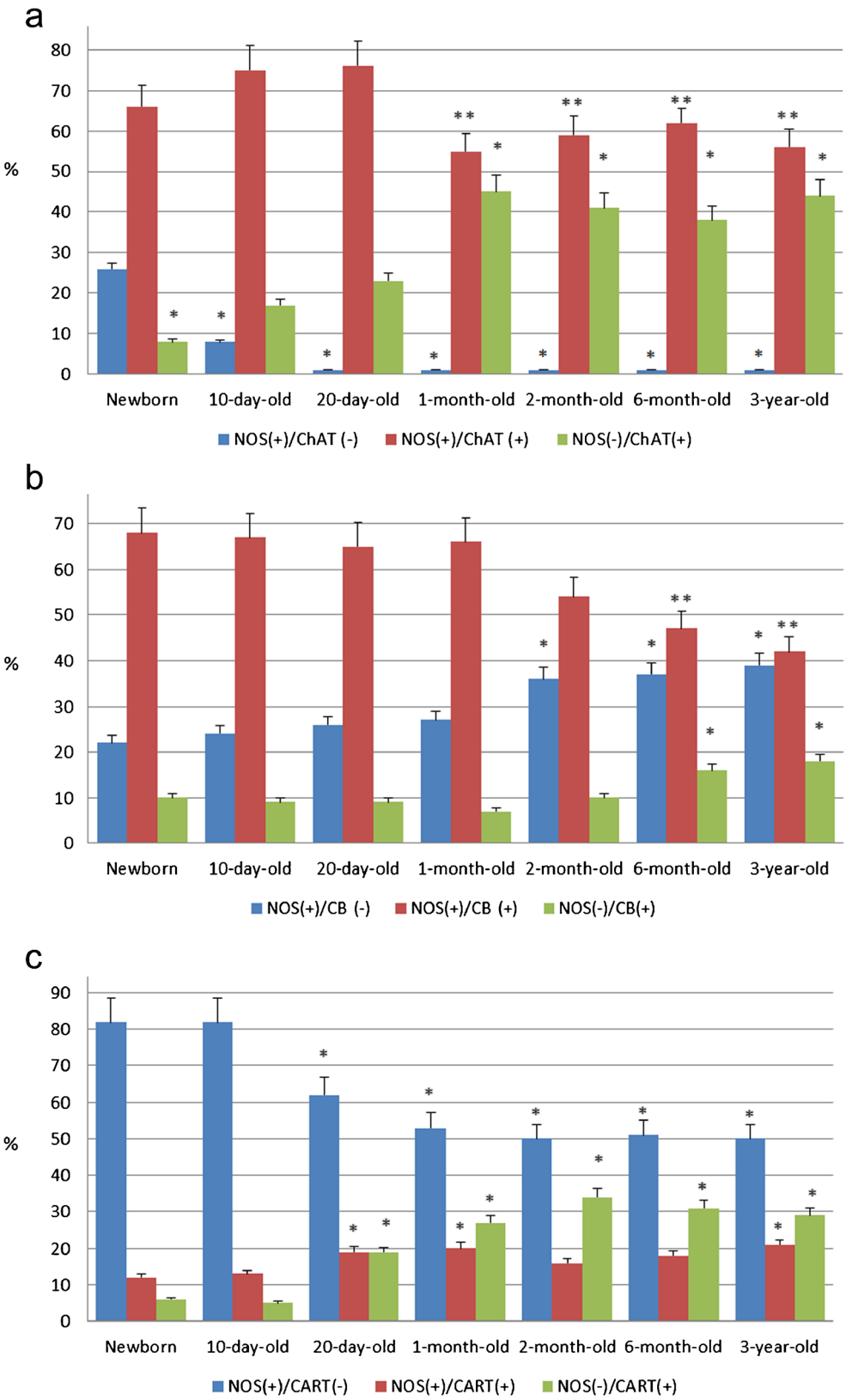

Fig. 2 Percentage of NOS(+)/ChAT(−), NOS(+)/ChAT(+), NOS(−)/ChAT(+) SPN (**a**), NOS(+)/CB(−), NOS(+)/CB(+), NOS(−)/CB(+) SPN (**b**), NOS(+)/CART(−), NOS(+)/CART(+), NOS(−)/CART(+) SPN (**c**) in the nucl.ILp of the Th2 SC segment in rats of different ages. The error bars represent SEM (*$p < 0.01$, when comparing newborn, **$p < 0.05$, when comparing 20-day-old rats)

The percentage of nNOS(+)/CART(+) SPN increased from 12 ± 1.7% in newborn to 29 ± 3.6% in 20-day-old rats (statistically significant differences, $p < 0.001$) (Fig. 6b). The proportion of nNOS(+)/CART(−) neurons decreased from 62 ± 5.6% in 10-day-old to 33 ± 4.1% in 1-month-old rats ($p < 0.001$).

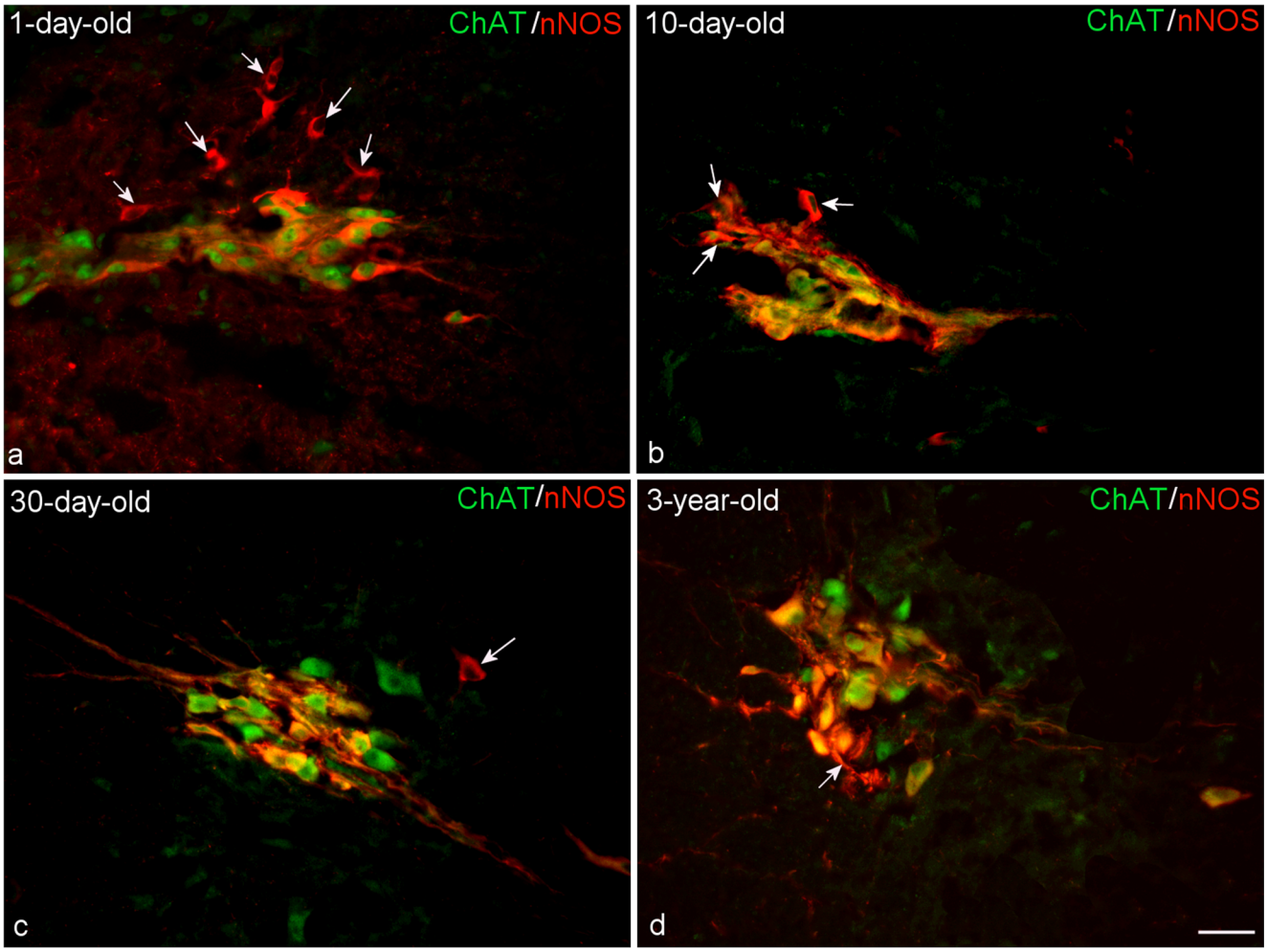

Fig. 3 Fluorescence micrographs of ChAT (green) and nNOS (red) immunoreactivity in the SC of newborn (**a**), 10-day-old (**b**), 30-day-old (**c**), 3-year-old (**d**) rats. nNOS (+)/ChAT (−) neurons are indicated by arrows. Bar, 50 μm

Expression of nNOS by western blot analysis

In order to further measure the protein expressions of nNOS, total protein extracted from the SC were subjected to western blot analysis. A nNOS-IR band of 155 KD was present in extracts of SC but it was much more intense in newborns (Fig. 7). Densitometric analysis revealed that it significantly decreased in the first 10 days ($p < 0.05$). No statistically significant differences were found between 10-day-old and older age groups ($p > 0.05$).

Table 4 Percentages of nNOS(+)/ChAT(−), nNOS(+)/ChAT(+), nNOS(−)/ChAT(+) neurons in nucl.IC and nucl.ICpe of SC in rats of different ages ($n = 5$ in every age group)

Age	nucl.IC			nucl.ICpe		
	nNOS(+)/ChAT(−)	nNOS(+)/ChAT(+)	nNOS(−)/ChAT(+)	nNOS(+)/ChAT(−)	nNOS(+)/ChAT(+)	nNOS(−)/ChAT(+)
Newborn	35 ± 1.7	31 ± 2.5	34 ± 2.1	36 ± 2.5	31 ± 1.2	33 ± 2.6
10-day-old	32 ± 2.8	36 ± 2.4	32 ± 1.5	30 ± 2.2	34 ± 1.6	36 ± 2.5
20-day-old	33 ± 1.9	32 ± 2.5	35 ± 2.1	35 ± 2.3	33 ± 1.1	32 ± 1.1
1-month-old	36 ± 1.4	31 ± 2.3	33 ± 1.6	36 ± 2.5	33 ± 1.1	31 ± 1.3
2-month-old	32 ± 2.7	33 ± 1.5	35 ± 1.1	36 ± 1.5	31 ± 2.2	33 ± 1.8
6-month-old	33 ± 1.7	33 ± 1.5	34 ± 1.1	32 ± 1.5	34 ± 2.2	34 ± 2.8
3-year-old	34 ± 0.7	35 ± 1.5	31 ± 2.1	35 ± 1.5	34 ± 1.2	31 ± 1.8

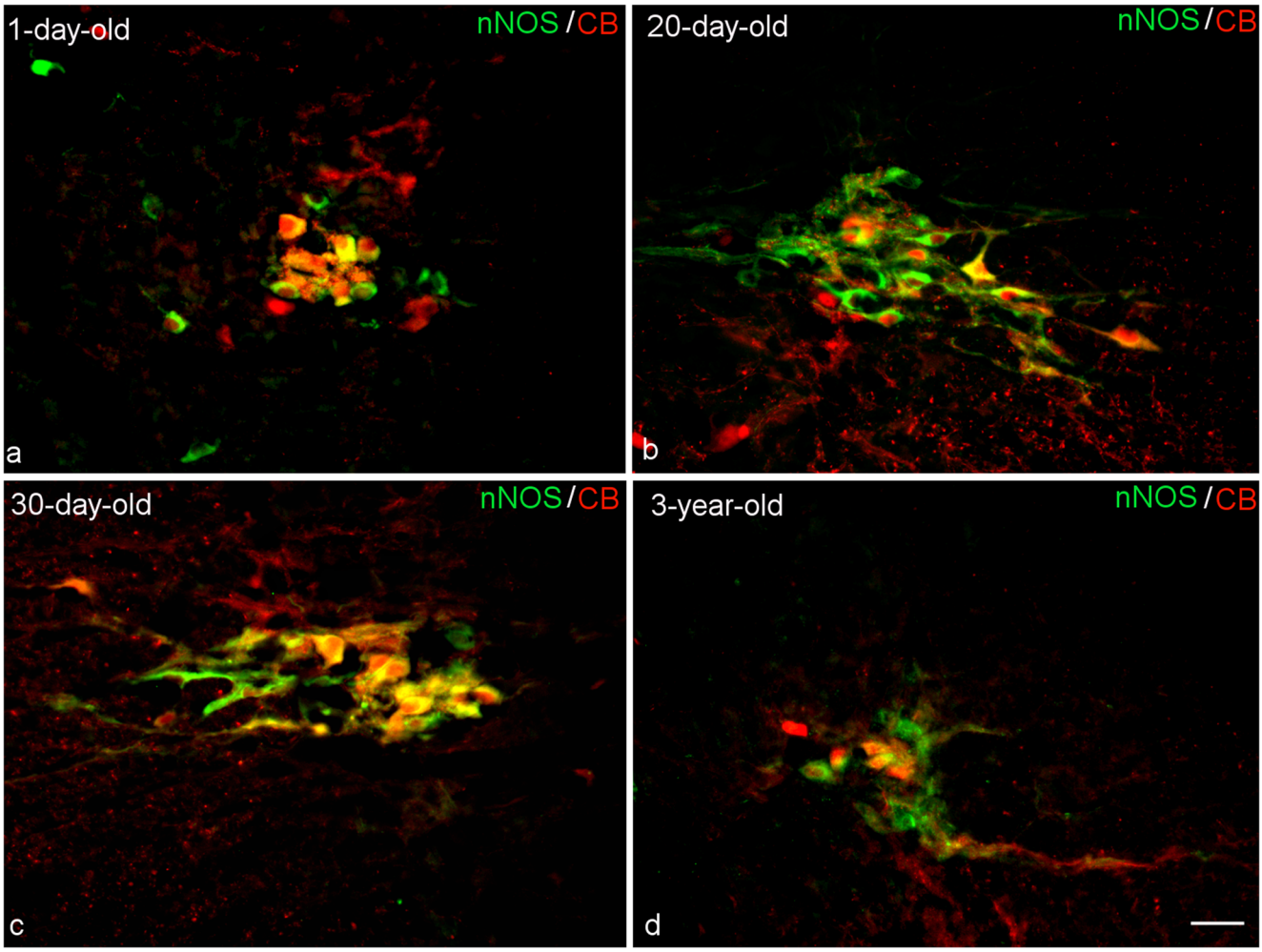

Fig. 4 Fluorescence micrographs of nNOS (green) and CB (red) immunoreactivity in the SC of newborn (**a**), 20-day-old (**b**), 30-day-old (**c**), 3-year-old (**d**) rats. Bar, 50 μm

Discussion

The present study reveals decreasing nNOS expression in SPN in rats during early postnatal development. We performed the current work on female rats since our previous study of nNOS expression in afferent and sympathetic ganglia in the rat development was also done on female animals (Masliukov et al. 2014). Previously, we studied morphology of neurons in the SC of both sexes and we did not observe gender differences (Porseva et al. 2014, 2015).

Somatic motoneurons and autonomic preganglionic neurons are generated synchronously in a single, ventrolaterally located column in the intermediate zone during the embryonic days 11–12 and express ChAT. At embryonic day 17, these autonomic motor neurons reache their final positions in the middle portion of the intermediate zone of SC (Phleps et al. 1991). SPN became NADPH-d- (and presumably nNOS) positive early in their development, as they were migrating toward their adult positions (Wetts et al. 1995).

By our data, even in newborns, nNOS-IR neurons were located in the intermediate gray matter of the SC in four groups corresponding to the four nuclei, the ILp, ILf, IC, and ICpe. The largest percentage of nNOS-IR neurons was located in the ILp. IC and ICpe contain slightly higher percentages of nNOS-IR SPN in the neonate when compared with the adult. Our findings are in accordance with previous data concerning the total distribution of SPN in the SC and its changes in the early postnatal development (Pyner and Coote 1994).

Cross-sectional area of nNOS-IR SPN enlarges in the first 10 days of life in rats. However, an increase of soma size in sympathetic and enteric ganglia goes more slowly. The cross-sectional areas of sympathetic neurons become similar to adult parameters at the end of 20–30 days (Masliukov et al. 2012) and in the enteric ganglia maturation of neurons finishes only at the end of the second month of life (Masliukov et al. 2017).

However, we found that in neonatal animals, the largest percentage of neurons was nNOS-IR and a small part of the neurons was ChAT(−) at the same time. During the first month

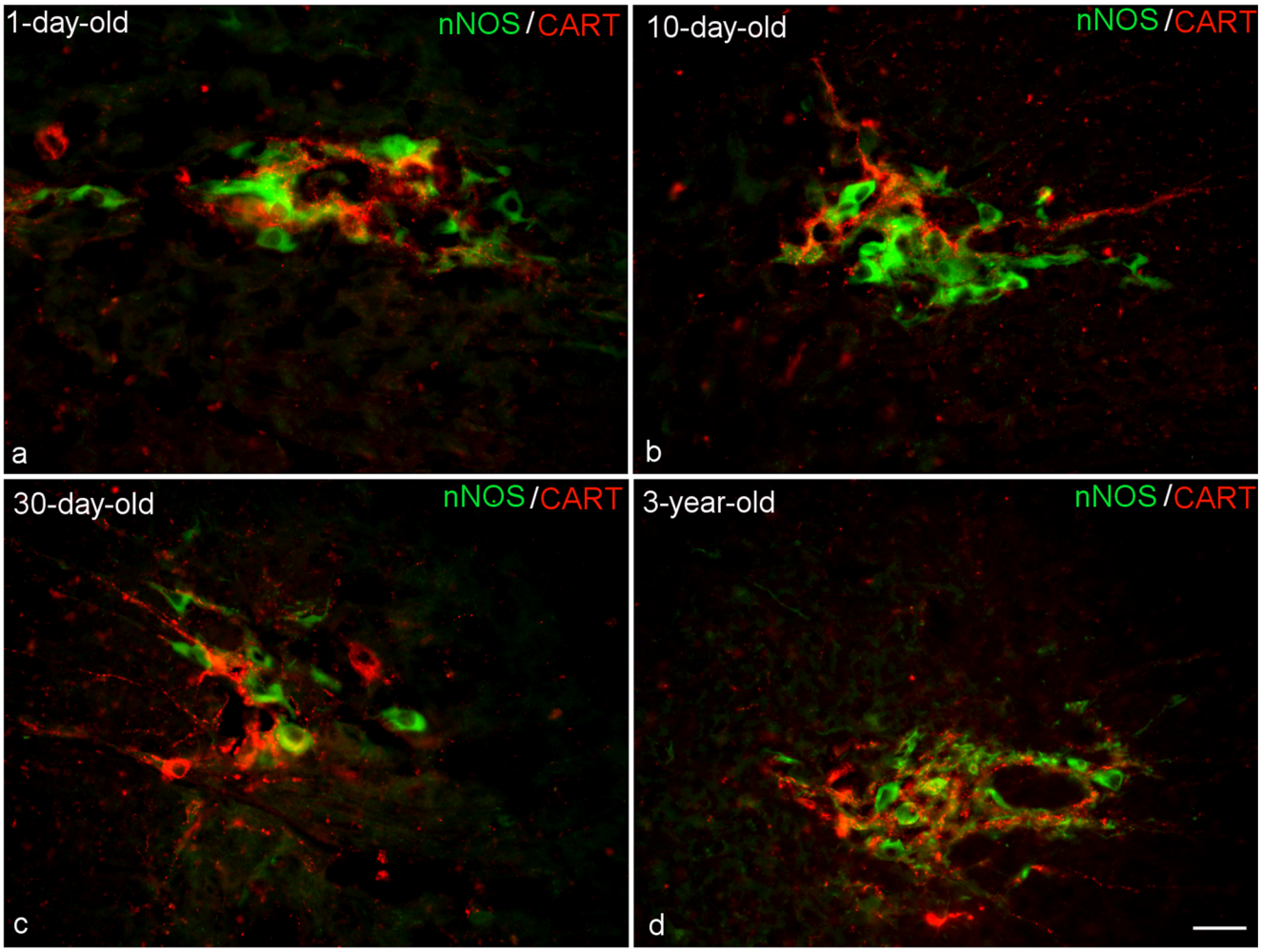

Fig. 5 Fluorescence micrographs of nNOS (green) and CART (red) immunoreactivity in the SC of newborn (**a**), 10-day-old (**b**), 30-day-old (**c**), 3-year-old (**d**) rats. Bar, 50 μm

of life, the proportion of nNOS-IR neurons decreased significantly, while the proportion of ChAT-IR neurons increased. In 1-month-old rats, 45% of SPN were nNOS(−). This portion remained almost unchanged afterwards including aged rats. We also confirmed the immunohistochemical data by western blot analysis where nNOS expression considerably decreased in the first 10 days of life.

Some literature data also point to a transient overexpression of nNOS in both the neuropil and specific neuronal populations of the developing cerebral cortex (Judas et al. 1999). NO has been implicated in various forms of neuronal remodeling and plasticity. For example, NO is necessary for both activity-mediated synapse formation (Nikonenko et al. 2003) and for the expression of neuroplasticity-associated protein expression (Gallo and Iadecola 2011). NO could nitrosylate different proteins, whereby it could modulate dendrite outgrowth during development (Zhang et al. 2010). nNOS inhibition, during development, leads to disturbances in dendrite morphology and to a reduction in synapse number (Sanchez-Islas and Leon-Olea 2004).

Nevertheless, in the autonomic ganglia, the patterns of nNOS and ChAT expression are different. Increased level of nNOS expression is also observed during development of the enteric ganglia. In the guinea pig's small intestine, the proportion of nNOS-expressing neurons decreases during postnatal development. The circular smooth muscle of the intestine appears to receive innervation from nNOS(+) fibers prior to ChAT(+) fibers (Patel et al. 2010). In contrast, in newborn rodents, the quantity of NADPH-d-positive preganglionic fibers in sympathetic ganglia is quite small and the number of fibers increased during early postnatal development (Emanuilov et al. 2008).

A number of contradictory studies have shown that NO could regulate neurotransmitter release. NO increases the efficacy of ganglionic synaptic cholinergic transmission and produces prolonged potentiation of ganglionic transmission in the chick ciliary ganglion and rat sympathetic superior cervical ganglion (Southam et al. 1996; Alkadhi et al. 2005). Furthermore, NO could also affect the expression of postsynaptic receptors to acetylcholine (Godfrey and Schwarte 2010).

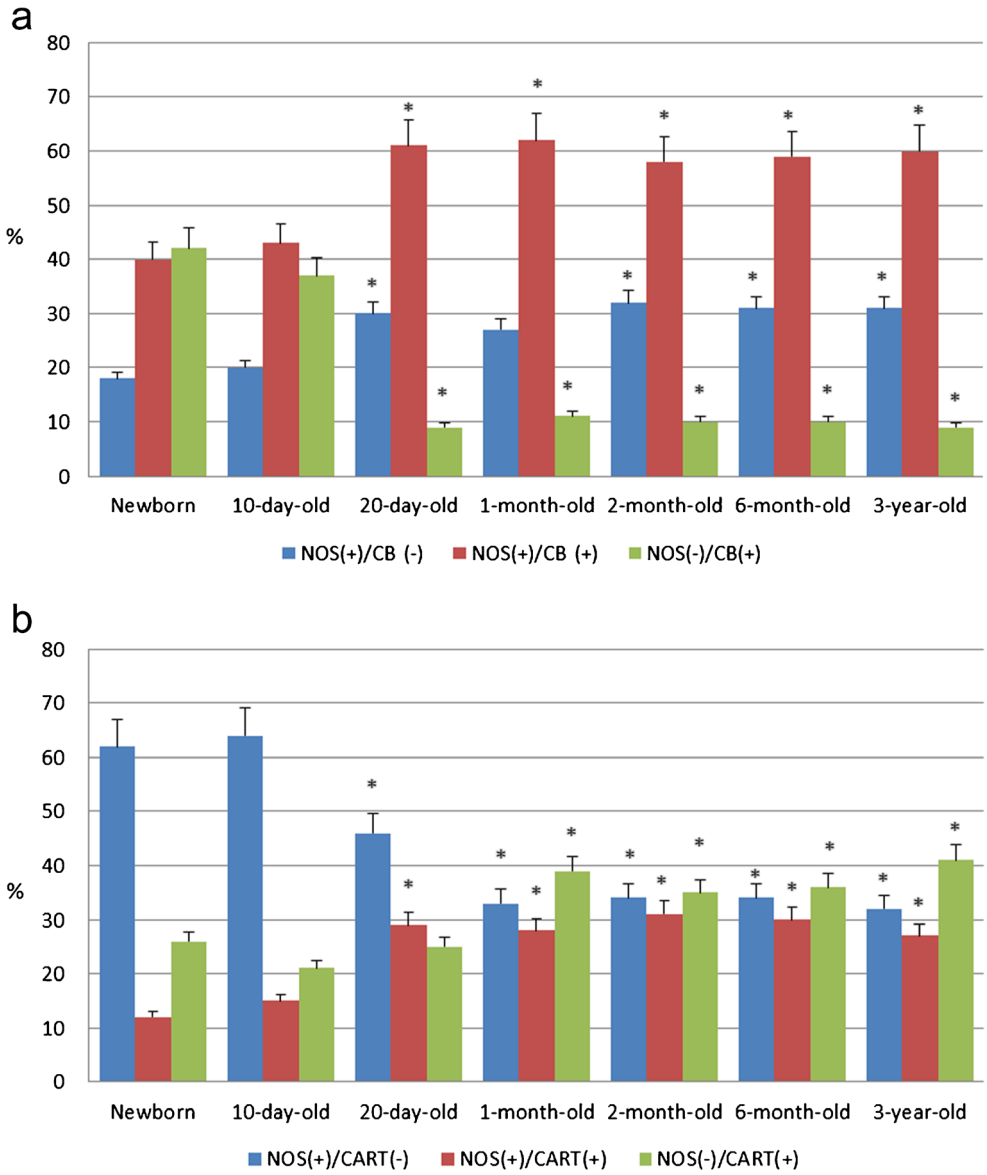

Fig. 6 Percentage of nNOS(+)/CB(−), nNOS(+)/CB(+), nNOS(−)/CB(+) SPN (**a**) and nNOS(+)/CART(−), nNOS(+)/CART(+), nNOS(−)/CART(+) SPN (**b**), in the nucl.IC of the Th2 SC segment in rats of different ages. The error bars represent SEM (*$p < 0.05$ (**a**), *$p < 0.001$ (**b**) when comparing to 10-day-old rats)

From other studies, NO reduces the evoked release of acetylcholine from the mouse motor nerve terminal (Yakovleva et al. 2013; Mukhutdinova et al. 2018).

In newborns, the amplitude of sympathetic nerve discharge is low and it may be explained by low efficacy of cholinergic synapses in sympathetic ganglia (Masliukov et al. 2000). Early synapses are weak, fatigue rapidly and display little spontaneous activity (Rubin 1985). In the early development, the amplitude of synaptic potentials in sympathetic ganglia increases and acetylcholine current densities double during the period when most of the synapses are forming (Gardette et al. 1991). In paravertebral sympathetic ganglia, there is a rapid increase in the number of ultrastructurally detectable synapses during fetal and neonatal development (Smolen and Raisman 1980). Thus, increase of nNOS/ChAT colocalization in the first weeks of life may reflect maturation of synaptic transmission during development. We suggest that the expression of ChAT in SPN in the early postnatal development is affected by the targets—sympathetic ganglionic neurons.

So, we can also suggest the dual role of NO in the development of autonomic SPN. It acts as a possible trophic factor and is capable of mediating interactions between SPN and ganglionic neurons before synapse formation or even physical contacts have occurred. Also, NO regulates acetylcholine release from presynaptic fibers and facilitates cholinergic neurotransmission in sympathetic ganglia.

Some nNOS-IR SPN also colocalized CART and CB. We found that the percentage of NOS(+)/CB(+) neurons decreased in the development. These data are in accordance with our previous findings about the decrease of CB expression in sympathetic ganglia of rats and cats (Masliukov et al. 2012,

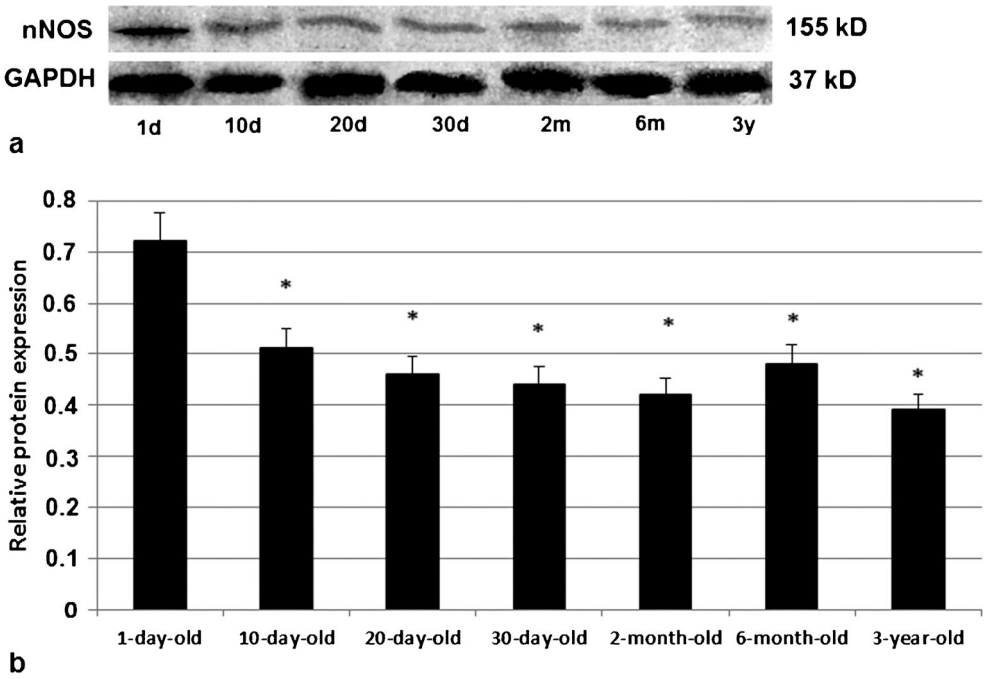

Fig. 7 Representative immunoblot bands of nNOS and GAPDH in the SC of newborn (1 day), 10-day-old (10 day), 20-day-old (20 day), 30-day-old (30 day), 2-month-old (2 m), 6-month-old (6 m), 3-year-old (3 year) rats (**a**). The data analysis of nNOS expression in the spinal cord of rats of different ages by Western blot (**b**). All data represented a relative quantification to internal control GAPDH. *$p < 0.05$ compared to newborns

2015). In mature neurons, calcium-binding proteins are involved in numerous functions, including cell signaling, calcium uptake and transport, cell motility, and intracellular calcium buffering. CB may protect neurons against large fluctuations in free intracellular Ca^{2+} and may prevent cell death (Andressen et al. 1993; Schwaller 2012). Possibly, CB is necessary to establish new synaptic contacts between axons of principal ganglionic neurons and target organs, preganglionic fibers and principal ganglionic neurons. (Siechen et al. 2009; Heiman and Shaham 2010). Thus, decrease in CB and nNOS expression in SPN may be explained by their role in the early development of autonomic neurons.

Meanwhile, the proportion of nNOS-IR neurons decreases when compared to nNOS(−)/CART(+) cells and it is very similar to changes of nNOS/ChAT colocalization. A substantial fraction of CART-IR SPN may be involved in cardiovascular regulation, because about 40% of CART-IR neurons in the ILp express Fos in response to a hypotensive stimulus. In the SC, low doses of CART potentiate the hypertension and tachycardia produced by intrathecal glutamate, and, at higher doses, the peptide itself can increase mean arterial pressure and heart rate (Scruggs et al. 2005). Thus, we can suggest that the process of increasing CART-IR and ChAT-IR in SPN may correspond with the elevation of heart rate and arterial blood pressure in the early period of postnatal development.

Conclusions

In summary, the present study provides further insight into the development of SPN in rats. In young and adult rats, the majority of SPN is nNOS-IR. In the development, the percentage of nNOS-IR neurons colocalizing CB neurons decreases, but the proportion of nNOS-IR neurons colocalizing ChAT and CART increases. The information provided in this study will also serve as a basis for future studies that investigate the mechanisms underlying the development of sympathetic neurons.

Funding information This work was supported by the RFBR (N 16-04-00538) grant.

Compliance with ethical standards

All animal procedures were approved by the Institutional Animal Care and Use Committee of the Yaroslavl State Medical University and were conducted in accordance with the "Guide for the Care and Use of Laboratory Animals" (NIH Publication No. 85–23, revised 1996) as well as the relevant Guidelines of the Russian Ministry of Health for scientific experimentation on animals.

References

Alkadhi KA, Alzoubi KH, Aleisa AM (2005) Plasticity of synaptic transmission in autonomic ganglia. Prog Neurobiol 75:83–108

Anderson CR (1992) NADPH diaphorase-positive neurons in the rat spinal cord include a subpopulation of autonomic preganglionic neurons. Neurosci Lett 139:280–284

Andressen C, Blumcke I, Celio MR (1993) Calcium-binding proteins: selective markers of nerve cells. Cell Tissue Res 271:181–208

Barber RP, Phelps PE, Houser CR, Crawford GD, Salvaterra PM, Vaughn JE (1984) The morphology and distribution of neurons containing choline acetyltransferase in the adult rat spinal cord: an immunocytochemical study. J Comp Neurol 229:329–346

Cossenza M, Socodato R, Portugal CC, Domith IC, Gladulich LF, Encarnação TG, Calaza KC, Mendonça HR, Campello-Costa P, Paes-de-Carvalho R (2014) Nitric oxide in the nervous system: biochemical, developmental, and neurobiological aspects. Vitam Horm 96:79–125

Dawson TM, Dawson VL (2018) Nitric oxide signaling in neurodegeneration and cell death. Adv Pharmacol 82:57–83

Dawson TM, Bredt DS, Fotuhi M, Hwang PM, Synder SH (1991) Nitric oxide synthase and neuronal NADPH diaphorase are identical in brain and peripheral tissues. Proc Natl Acad Sci U S A 88:7797–7801

Dun NJ, Dun SL, Kwok EH, Yang J, Chang J (2000) Cocaine- and amphetamine-regulated transcript immunoreactivity in the rat sympathoadrenal axis. Neurosci Lett 283:97–100

Emanuilov AI, Korzina MB, Archakova LI, Novakovskaya SA, Nozdrachev AD, Masliukov PM (2008) Development of the NADPH-diaphorase-positive neurons in the sympathetic ganglia. Ann Anat 190:516–524

Fenwick NM, Martin CL, Llewellyn-Smith IJ (2006) Immunoreactivity for cocaine- and amphetamine-regulated transcript in rat sympathetic preganglionic neurons projecting to sympathetic ganglia and the adrenal medulla. J Comp Neurol 495:422–433

Gallo EF, Iadecola C (2011) Neuronal nitric oxide contributes to neuroplasticity-associated protein expression through cGMP, protein kinase G, and extracellular signal-regulated kinase. J Neurosci 31:6947–6955

Gardette R, Listerud MD, Brussaard AB, Role LW (1991) Developmental changes in transmitter sensitivity and synaptic transmission in embryonic chicken sympathetic neurons innervated in vitro. Dev Biol 147:83–95

Gibbs SM (2003) Regulation of neuronal proliferation and differentiation by nitric oxide. Mol Neurobiol 27:107–120

Godfrey EW, Schwarte RC (2010) Nitric oxide and cyclic GMP regulate early events in agrin signaling in skeletal muscle cells. Exp Cell Res 316:1935–1945

Gonsalvez DG, Kerman IA, McAllen RM, Anderson CR (2010) Chemical coding for cardiovascular sympathetic preganglionic neurons in rats. J Neurosci 30:11781–11191

Grkovic I, Anderson CR (1997) Calbindin D28K-immunoreactivity identifies distinct subpopulations of sympathetic pre- and postganglionic neurons in the rat. J Comp Neurol 386:245–259

Heiman MG, Shaham S (2010) Twigs into branches: how a filopodium becomes a dendrite. Curr Opin Neurobiol 20:86–91

Judas M, Sestan N, Kostović I (1999) Nitrinergic neurons in the developing and adult human telencephalon: transient and permanent patterns of expression in comparison to other mammals. Microsc Res Tech 45:401–419

Masliukov PM, Fateev MM, Nozdrachev AD (2000) Age-dependent changes of electrophysiologic characteristics of the stellate ganglion conducting pathways in kittens. Auton Neurosci 83:12–18

Masliukov PM, Korobkin AA, Nozdrachev AD, Timmermans JP (2012) Calbindin-D28k immunoreactivity in sympathetic ganglionic neurons during development. Auton Neurosci 167:27–33

Masliukov PM, Emanuilov AI, Madalieva LV, Moiseev KY, Bulibin AV, Korzina MB, Porseva VV, Korobkin AA, Smirnova VP (2014) Development of nNOS-positive neurons in the rat sensory and sympathetic ganglia. Neuroscience 256:271–281

Masliukov PM, Emanuilov AI, Moiseev K, Nozdrachev AD, Dobrotvorskaya S, Timmermans JP (2015) Development of non-catecholaminergic sympathetic neurons in para- and prevertebral ganglia of cats. Int J Dev Neurosci 40:76–84

Masliukov PM, Emanuilov AI, Nozdrachev AD (2016) Developmental changes of neurotransmitter properties in sympathetic neurons. Adv Gerontol 29:442–453

Masliukov PM, Moiseev K, Budnik AF, Nozdrachev AD, Timmermans JP (2017) Development of calbindin- and calretinin-immunopositive neurons in the enteric ganglia of rats. Cell Mol Neurobiol 37:1257–1267

Meller ST, Gebhart GF (1993) Nitric oxide (NO) and nociceptive processing in the spinal cord. Pain 52:127–136

Mukhutdinova KA, Kasimov MR, Giniatullin AR, Zakyrjanova GF, Petrov AM (2018) 24S-hydroxycholesterol suppresses neuromuscular transmission in SOD1(G93A) mice: a possible role of NO and lipid rafts. Mol Cell Neurosci 88:308–318

Nikonenko I, Jourdain P, Muller D (2003) Presynaptic remodeling contributes to activity-dependent synaptogenesis. J Neurosci 23:8498–8505

Patel BA, Dai X, Burda JE, Zhao H, Swain GM, Galligan JJ, Bian X (2010) Inhibitory neuromuscular transmission to ileal longitudinal muscle predominates in neonatal guinea pigs. Neurogastroenterol Motil 22:909–918

Petho G, Reeh PW (2012) Sensory and signaling mechanisms of bradykinin eicosanoids platelet-activating factor and nitric oxide in peripheral nociceptors. Physiol Rev 92:1699–1775

Phelps PE, Barber RP, Vaughn JE (1991) Embryonic development of choline acetyltransferase in thoracic spinal motor neurons: somatic and autonomic neurons may be derived from a common cellular group. J Comp Neurol 307:77–86

Porseva VV, Shilkin VV, Strelkov AA, Masliukov PM (2014) Subpopulation of calbindin-immunoreactive interneurons in the dorsal horn of the mice spinal cord. Tsitologiia 56:612–618

Porseva VV, Shilkin VV, Krasnov IB, Masliukov PM (2015) Calbindin-D28k immunoreactivity in the mice thoracic spinal cord after space flight. Int J Astrobiol 14:555–562

Prast H, Philippu A (2001) Nitric oxide as modulator of neuronal function. Prog Neurobiol 64:51–68

Pyner S, Coote JH (1994) A comparison between the adult rat and neonate rat of the architecture of sympathetic preganglionic neurones projecting to the superior cervical ganglion stellate ganglion and adrenal medulla. J Auton Nerv Syst 48:153–166

Rubin E (1985) Development of the rat superior cervical ganglion: initial stages of synapse formation. J Neurosci 5:697–704

Sanchez-Islas E, Leon-Olea M (2004) Nitric oxide synthase inhibition during synaptic maturation decreases synapsin I immunoreactivity in rat brain. Nitric Oxide 10:141–149

Schmidt HHHW, Gagne GD, Nakane M, Pollock JS, Miller MF, Murad F (1992) Mapping of neural nitric oxide synthase in the rat suggests frequent co-localization with NADPH diaphorase but not with soluble guanylyl cyclases and novel paraneural functions for nitrinergic signal transduction. J Histochem Cytochem 40:1439–1456

Scruggs P, Lai CC, Scruggs JE, Dun NJ (2005) Cocaine- and amphetamine-regulated transcript peptide potentiates spinal glutamatergic sympathoexcitation in anesthetized rats. Regul Pept 127: 79–85

Schwaller B (2012) The use of transgenic mouse models to reveal the functions of Ca2+ buffer proteins in excitable cells. Biochim Biophys Acta 1820:1294–1303

Siechen S, Yang S, Chiba A, Saif T (2009) Mechanical tension contributes to clustering of neurotransmitter vesicles at presynaptic terminals. Proc Natl Acad Sci U S A 106:12611–12616

Smolen A, Raisman G (1980) Synapse formation in the rat superior cervical ganglion during normal development and after neonatal deafferentation. Brain Res 787:315–323

Snyder SH (1992) Nitric oxide: first in a new class of neurotransmitters. Science 257:494–496

Southam E, Charles SL, Garthwaite J (1996) The nitric oxide-cyclic GMP pathway and synaptic plasticity in the rat superior cervical ganglion. Br J Pharmacol 119:527–532

Wetts R, Vaughn JE (1994) Choline acetyltransferase and NADPH diaphorase are co-expressed in rat spinal cord neurons. Neuroscience 63:1117–1124

Wetts R, Phelps PE, Vaughn JE (1995) Transient and continuous expression of NADPH diaphorase in different neuronal populations of developing rat spinal cord. Dev Dyn 202: 215–228

Yakovleva OV, Shafigullin MU, Sitdikova GF (2013) The role of nitric oxide in the regulation of neurotransmitter release and processes of exo- and endocytosis of synaptic vesicles in mouse motor nerve endings. Neurochem J 7:103–110

Young HM, Cane KN, Anderson CR (2011) Development of the autonomic nervous system: a comparative view. Auton Neurosci 165: 10–27

Zhang P, Yu PC, Tsang AH, Chen Y, Fu AK, Fu WY, Chung KK, Ip NY (2010) S-nitrosylation of cyclin-dependent kinase 5 (cdk5) regulates its kinase activity and dendrite growth during neuronal development. J Neurosci 30:14366–14370